ACS OMEGA

Open Access

http://pubs.acs.org/journal/acsodf

Article

Tanning Wastewater Sterilization in the Dark and Sunlight Using *Psidium guajava* Leaf-Derived Copper Oxide Nanoparticles and Their Characteristics

Natrayan Lakshmaiya, Raviteja Surakasi, V. Swamy Nadh, Chidurala Srinivas, Seniappan Kaliappan, Velmurugan Ganesan, Prabhu Paramasivam,* and Seshathiri Dhanasekaran

Cite This: *ACS Omega* 2023, 8, 39680−39689

Read Online

ACCESS | Metrics & More | Article Recommendations

ABSTRACT: Employing *Psidium guajava* (*P. guajava*) extract from leaves, copper oxide nanoparticles (CuO NPs), likewise referred to as cupric oxide and renowned for their sustainable and harmless biogenesis, have the possibility of being useful for the purification of pollutants as well as for medicinal purposes. The current study examined the generated CuO NPs and their physical qualities by using ultraviolet−visible (UV) spectroscopy. The distinctive peak at 265 nm of the CuO NP production was originally seen. Additionally, an X-ray diffraction (XRD) investigation was conducted to identify the crystalline arrangement of the produced CuO NPs, and a Fourier transform infrared (FTIR) spectroscopy examination was performed to validate the functional compounds of the CuO NPs. Additionally, the synthesized nanoparticles' catalytic activities (wastewater treatment) were analyzed in dark and sunlight modes. The catalytic properties of CuO NPs in total darkness resulted in 64.21% discoloration, whereas exposure to sunshine increased the nanomaterials' catalyst performance to 92.31%. By lowering Cr(VI), Ni, Pb, Co, and Cd in sewage by proportions of 91.4, 80.8, 68.26, 73.25, and 72.4% accordingly, the CuO NP demonstrated its effectiveness as a nanosorbent. Total suspended solids (TSS), total dissolved solids (TDS), chemical oxygen demand (COD), biological demand for oxygen (BOD), and conductance were all successfully reduced by nanotreatment of tanning effluents, with proportion reductions of 93.24, 88.62, 94.21, 87.5, and 98.3%, correspondingly.

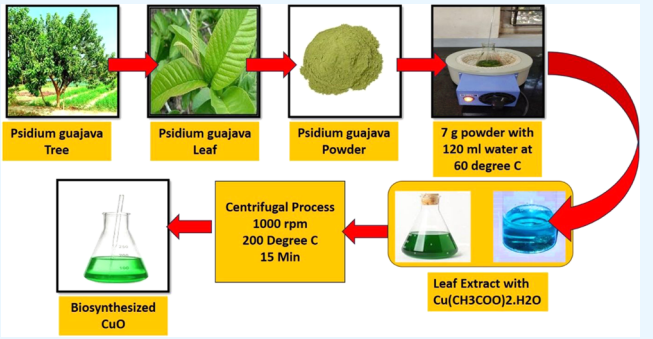

1. INTRODUCTION

Water is the first naturally occurring substance abundant on Earth, making up over 80% of the crust's moisture content. It is a vital part of the ecosystem of water and is used by humans for drinking, whether for household, commercial, or other purposes. On the planet, water molecules exist in three states: fluid, vapor, and solid. Whether directly or indirectly, without any special treatment, the industrial operations throughout the production process emitted both liquid and solid wastes that contaminated the water.[1] Among such water pollutants are harmful sulfides, chromite minerals, textile-related pollutants from azo colorants, and tiny quantities of metallic elements. The release of harmful substances and industrial waste into bodies of water seriously threatens aquatic life, vegetation, and people's health. Consuming large amounts of waste from factories may lead to tumors and other illnesses, including jaundice, cardiac arrest, and digestive issues. Most of the world's population now lives in underdeveloped nations without access to clean groundwater.[2] The World Health Organization (WHO) claimed that 854 million people worldwide did not have access to basic drinking water facilities in 2019 and that 160 million individuals relied on water from the ground. According to worldwide research, by 2026, at least two billion individuals will consume fluid contaminated by excrement.[3,4] These factors make sewage treatment and discharge regulation critical to meet water needs and maintain aquatic environments. Due to their varied chemical, physical, and physiological features, many investigators have proposed employing environmentally friendly techniques to biosynthesize nanoparticles of metals and oxides for water treatment. Nanotechnology has been extensively employed in the last 10 years in countless biological uses, including medication

Received: July 31, 2023
Accepted: September 25, 2023
Published: October 9, 2023

transport, diagnostics, antibacterial and carcinogenic activities, and numerous cancer therapies. Additionally, it can be used for wastewater treatment of petrochemical colors due to its diverse nanostructure and enormous dimension.[5]

Most of the particles are separated during the initial procedure, which typically consists of two phases, and biodegradable organic matter is removed by biological means during the second phase. Yet, there is still a sizable amount of phosphorus and nitrogen elements in second-generation sewage, which frequently cause pollution in aquatic systems.[6] This is accomplished by implementing secondary processes for wastewater to decrease phosphorus and nitrogen levels to 0.3 mg/L. The processes above rely on bacteria's ability to reduce phosphorus and nitrogen and biological and chemical mechanisms. Nevertheless, typical wastewater treatments have several drawbacks, including massive chemical usage, emissions of greenhouse gases, high operating and installation expenses, and high electricity consumption.[7,8] The disadvantage of disposing of sewage in a way that could lead to ecological problems occurs with the active sludge processing method, which is typically used in secondary processing. Ongoing population growth is anticipated to result in a steady rise in wastewater production, which might lead to a greater discharge of nutrients into the top layer of water. In the decades to come, there will be a need for additional sewer treatment plants, particularly tertiary wastewater treatment plants or advanced ones.[9,10] Since companies cannot pay the steadily rising expenditures on treatment amenities, certain emerging and lower-income nations have not invested in and upgraded treatment facilities at the same rate as urbanization and population growth.[11] However, another difficult problem for emerging nations is managing medical centers′ steadily growing operation and maintenance expenses. Therefore, it is crucial to create sewage treatment facilities that both are high-performing and require less capital. Several approaches were reported to extract nitrogen and phosphates from sewage, including using a hybrid adsorbent, ligand-based conjugated substances, membrane contactors, and tiny algae. Because of their advantages, phytoplanktons are increasingly used to remove nitrogen and phosphorus from sewage. The group of single-celled organisms known as microalgae is found in many aquatic habitats and ranges in dimension from a few to a couple of millimeters.[11−13]

Different approaches like hydrothermal, sol−gel, chemical response, coprecipitation, vapor depositing, laser treatment, electrodeposition, and bubbling are used to create metallic oxide nanomaterials. Due to their simpler advantages, psychological and chemical procedures are commonly used to synthesize and create various nanomaterials.[14] However, when metallic salt is converted into metal dioxide or metal oxide particles by chemical synthesis, hazardous substances that take the Gestalt of diminishing and stabilizing reagents are used. Such compounds have the potential to destroy the atmosphere as well as human beings. Nevertheless, the elevated temperature, severe pressure, and high energetic physical power requirements of the physiological techniques might harm large-scale manufacturing. This has contributed to the discovery of nontoxic and affordable methods for ecologically creating nanostructures that may be used by friendly and unicellular living things like yeast cells, bacteria, fungus microorganisms′ bacteria, and botanical extracts.[15,16] These synthesis methods have resulted in useful aggregates that may stabilize and reduce agents for nanoparticles generated during biosynthesis. These techniques lessen toxic consumption and offer insightful information on biologic compatibility, making them valuable for pharmacological and environmental objectives.

Copper oxide (CuO), a semiconductor material with a very small band gap of 1.7 eV, is also called cupric oxide. With the utilization of natural liquid extracts from plants, including the Malva sylvestris, aloe vera plant, Carica papaya, Glory superba, Sida acuta, *Citrus limon* and Ruellia tuberosa, several approaches were recently reported for the manufacture of CuO NPs utilizing a green biochemistry technique.[17] Due to the high concentration of pharmacologic components in *P. guajava* leaf extract, it is frequently used as a traditional medicine around the globe. Traditional applications of *P. guajava* fruits and leaves include the treatment of conditions, including obesity, diarrhea, high blood pressure, diarrhea, dermatological treatments, and wound rehabilitation in regions like Southeast Asia, Africa, South America, and Mesoamerica. The second-generation polyphenols and phenolic substances like flavonoids, mostly precursors of propranolol and have several pharmacological activities, including anticancer, antioxidant, antibacterial, and infectious action, are highly concentrated in the leaf of guava extracts.[18] Due to terpinene and phenol in plant leaf extracts, molecules of flavonoids produced from guava leaves can prevent Gramme+ and Gramme+ infections caused by bacteria. The research presented was novel since it was the first to describe using extracts of *P. guajava* leaf for pharmaceutical purposes.[19] The natural production of CuO NPs in this work uses aqueous extracts of leaves as reducing and capsizing agents. CuO nanoparticles (CuO NPs) are currently being extensively employed for study in the physiological and therapeutic domains; biological activity relies on the structure and dimensions of the nanomaterials. Additionally, biogenerated CuO NPs were effective in removing 85% of the dye and 28, 42, and 85% of the metals nickel (Ni), chromium (Cr), and lead (Pb) from the effluent of textiles. It has been demonstrated that several factors, including interaction duration, nanosorbent dosage, pH, and metallic ion levels, influence the removal of nickel, lead, and Cd (cadmium) in contaminated water using CuO, one of the most widely utilized nanomaterials.[20,21] Similar to this, myco-produced MgO NPs have demonstrated exceptional effectiveness in the purification of dyeing effluents, documenting more than 95% color elimination ability, around 97% elimination of chromium particles, and a decline in the electrical conductivity and chemical constitution of the disinfected water, such as biological demand for oxygen (BOD), total dissolved solids (TDS), total suspended solids (TSS), and chemical oxygen demand.[22] Consequently, the use of environmentally friendly products that have been biocompatible with heavy metal removal and sewage treatment in factories is acceptable. Such are the major obstacles to overcoming the chemical compounds′ drawbacks. Their significance is amplified whenever these new substances exhibit antibacterial and antifungal abilities.

One of the study's major innovations is the use of *P. guajava* leaves as a natural source for synthesizing copper oxide nanoparticles. This environmentally friendly technology reduces reliance on traditional chemical synthesis techniques and promotes sustainability. This study aims to determine how well copper oxide nanoparticles (CuO NPs) from *P. guajava* leaves can clean tanning wastewater. The objective is to offer a

https://doi.org/10.1021/acsomega.3c05588
ACS Omega 2023, 8, 39680−39689

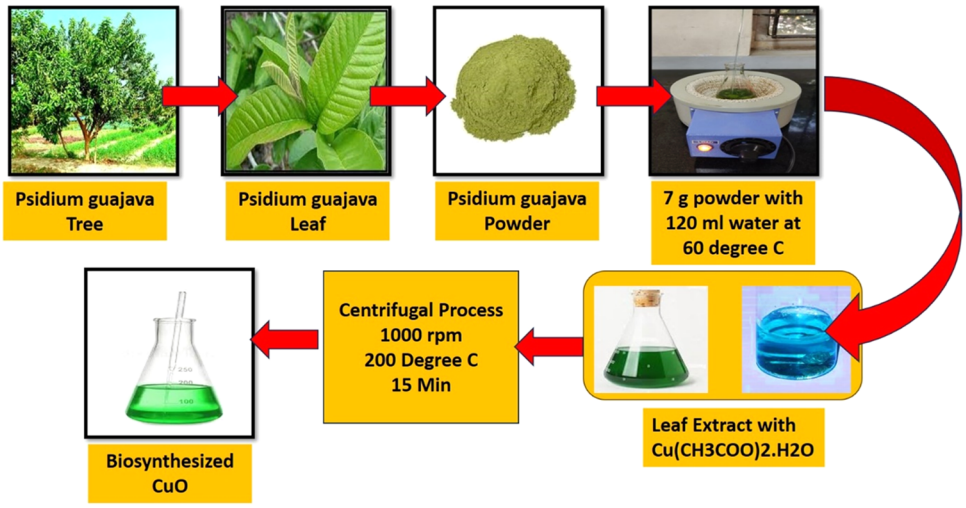

Figure 1. Graphical representation of biosynthesized CuO NPs from *P. guajava* leaf.

fresh and efficient method for sterilizing and cleaning the complicated wastewater that tanning operations produce, which contains a variety of contaminants. Another goal is to contrast the sterilizing effectiveness of CuO NPs made from *P. guajava* leaf under dark and light illumination. It makes it easier to assess how different light sources affect the nanoparticles' photocatalytic capabilities and their capacity to destroy bacteria. This entails assessing the likelihood that nanoparticles will be released into the environment and comprehending their long-term consequences for ecosystems. UV spectroscopy, dynamic light scattering (DLS), X-ray diffraction (XRD), Fourier transform infrared (FTIR), and transmission electron microscopy (TEM) were used to characterize the green-synthesized CuO NPs. Additionally, the ability of CuO as a nanosorbent to decolorize and enhance the physicochemical properties of effluents from tanneries was assessed.

2. EXPERIMENTAL WORKS

2.1. Materials. Science Laboratory Spaces in Chennai, Tamil Nadu, India, provided the testing compounds and copper acetate of standard academic quality. Deionized water was used throughout the whole trial. Clean *P. guajava* plant leaves were taken from a hamlet close to Alagappa University in Karaikudi, Tamil Nadu, India. Ten grams of plant material was eliminated, cleaned using double-deionized water 2−3 times to remove any remaining dust fragments, and then allowed to air-dry in sunlight. The leaves were subsequently separated into tiny fragments, placed in a 250 mL Erlenmeyer flask with 100 mL of distilled water, and heated for 20 min at a temperature above 60 °C. The Whatman filtering material (No. 1) enabled the extract from the leaves to pass throughout. The extracted leaves were subsequently stored in a cold area for future research.

2.2. Green Synthesis of CuO NPs. The *P. guajava* plant leaves were gathered, cleaned with tap water three times to remove foreign material, dried at 50 °C to make ash, and ground into a fine powder. Following that, 7 g of the produced powder was combined with 120 mL of purified water and heated at 60 °C for 1 h. The mixture was centrifuged at 1200 rpm for 15 min, and the resulting liquid was gathered and employed in the following manner for the biosynthesis of CuO NPs: Cu $(CH_3COO)_2$, 100 g. The final amount of 5 mM H_2O was obtained by dissolving it in 100 mL of pure water, mixing it thoroughly, and then adding botanical extract via drops to make 120 mL total.

Drops of 1N sodium hydroxide have been added to the prior combination and stirred for 60 min to get the pH level to 7. The green precipitation was obtained by centrifuging it at 1200 rpm for 15 min, washing it three times with purified water, and then drying it for three h at 300 °C. The effective synthesis of CuO NPs is shown by creating a greenish color after combining the liquid extract with Cu $(CH_3COO)_2$. H_2O and setting the pH at 7. Conversely, a plant's water-based extract showed no color changes under identical conditions and with no metallic precursors. Similarly, the greenish color was produced by combining copper sulfate with guajava plant leaf extract in water. The initial indication of CuO NP biosynthesis is a visual assessment of a water extract following its interaction with a metallic precursor. According to prior reports, the vibrations and resonance of positively charged particles on the NP surfaces may cause the color shift from colorless to green. Figure 1 shows a graphical representation of biosynthesized CuO NPs.

2.3. Characterization of Biosynthesised CuO NPs. Utilizing UV−vis spectral analysis, the energy of the band gap was identified at wavelengths from 240 to 750 nm, and the biosynthesis of CuO NPs was verified. To find the highest surface plasmon resonance values, 2 mL of the synthesized mixture was placed in a crystal cuvette, and its absorption was recorded regularly. A Jasco 6300 FTIR spectrometer was used to determine the functional sections of the CuO NPs produced during biosynthesis. Using an XRD diffractometer, the stage of crystalline development of the synthesized CuO NPs was established.

According to Debye−Scherrer's eq 1 and XRD examination, the mean size of the crystals of plant-based CuO NPs is as follows: SEM studies were used to examine the superficial morphological features of the generated CuO NPs. Employing TEM, we investigated the particulate dimensions of CuO NPs. DLS spectroscopy was used to determine the CuO NP dimension distribution. The synthesized CuO NPs were suspended in an extremely clean solvent to prevent a shadow from appearing on the data throughout the dispersion evaluation

https://doi.org/10.1021/acsomega.3c05588
ACS Omega 2023, 8, 39680−39689

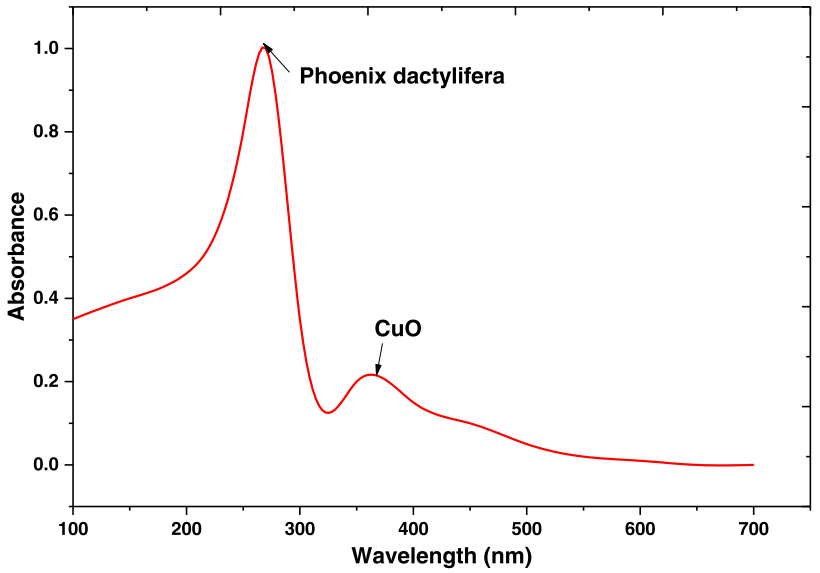

Figure 2. UV spectroscopy of biosynthesized CuO nanoparticles.

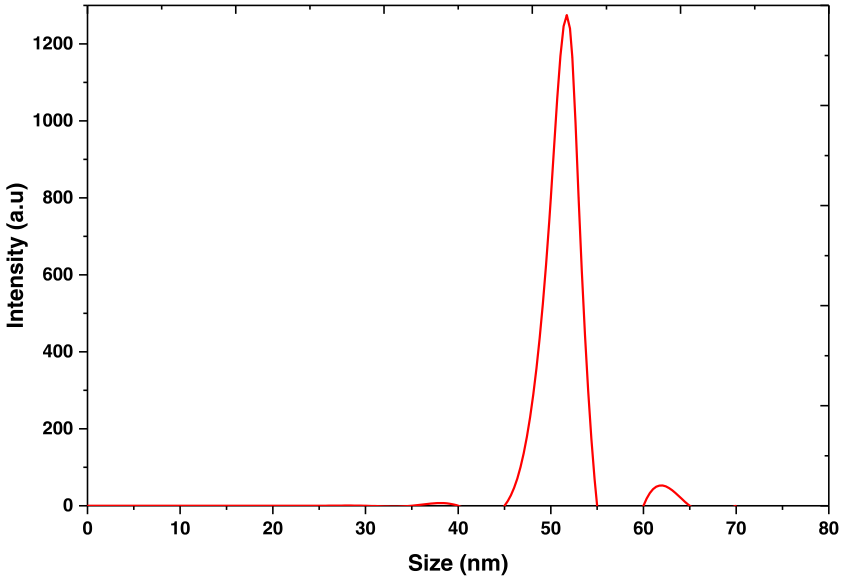

Figure 3. Dynamic light scattering analysis of biosynthesized CuO nanoparticles.

$$\text{average crystallite size} = \frac{0.94 \times 1.54}{\beta \cos \theta} \quad (1)$$

wherein 1.54 is the X-ray wavelength, 0.94 is the Scherrer constant, β is the dispersion angle, and θ is the complete breadth of the dispersion spike at half-maximum.

2.4. Wastewater Treatment. The deterioration and discoloration of gasoline tanners' waterways at different concentration levels (0.4, 0.8, 1.2, and 1.6 mg/mL) with different exposure times (30, 60, 90, 120, 150, 180, 210, 160, 180, and 210 min) in both dark and sunlight incubating conditions were used to test the catalytic capacity of green-synthesized CuO NPs. The pH of the treated liquid was determined both before and after the catalysis investigation, which was conducted at a temperature of 40 °C. A medium-sized bubble dispersion system and a low-pressure, high-efficiency compressor were used to aerate a catalytic batch during creation.

In order to achieve the absorption/desorption point of equilibrium, an established quantity of tanner effluent was combined with a certain amount of synthesized CuO NPs and exposed to 200 rpm swirling for 15 min before the test. A certain set of tests was incubated in the dark, while another set was similarly incubated with sunlight exposure. Three copies of all treatments were carried out. The color removal proportions (%) were calculated by taking 1 mL of the solution at certain intervals, centrifuging it for 5 min at 12,000 rpm, and measuring absorbance at 500 nm with a spectrum analyzer. The aforementioned formula was used to obtain decolorization proportions (%).

$$\textit{decolorization percentage}\ (\%) = \frac{C_0 - C_t}{C_0} \times 100 \quad (2)$$

where C_t is the absorption rate at a certain time and C_0 is the absorption at 0 h (before the test).

https://doi.org/10.1021/acsomega.3c05588
ACS Omega 2023, 8, 39680−39689

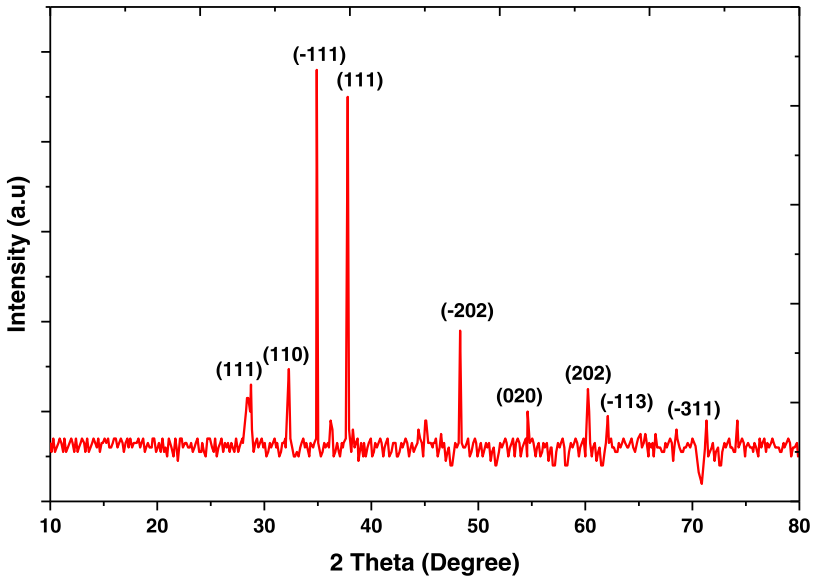

Figure 4. XRD pattern of biosynthesized CuO nanoparticles.

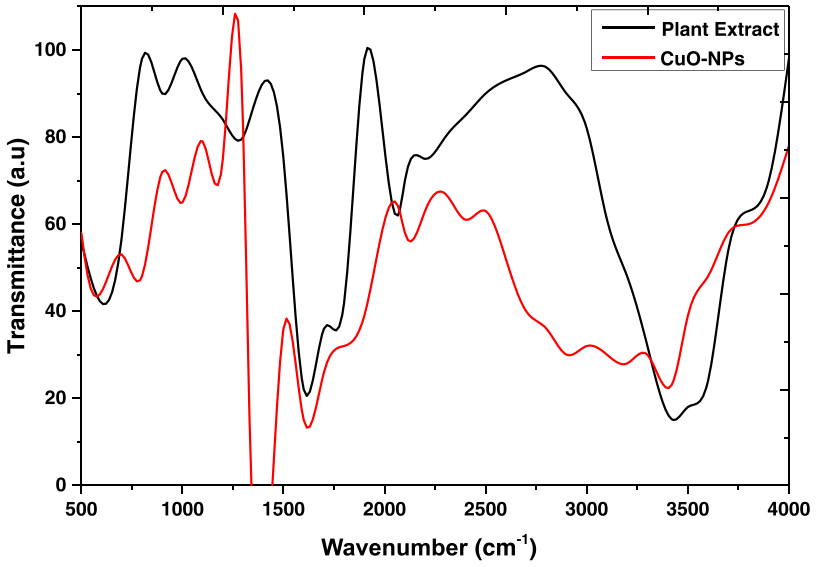

Figure 5. FTIR structure of biosynthesized CuO nanoparticles along with their plant extract.

3. RESULT AND DISCUSSION

3.1. UV−Vis Spectroscopy. UV−vis spectroscopy is used to assess the color shift by NP production and to find the highest surface plasmon resonance (SPR). By using intense light at a certain wavelength, the electrons liberated on the NP surfaces attract one another, producing the greatest peak. The greatest peak (Figure 2) in the present investigation was found at a wavelength of 265 nm, equivalent to the highest SPR of CuO NPs. The greatest SPR of CuO NPs made with Vitex negundo leaf extract in water was seen at 274 nm, consistent with the outcome. Additionally, the CuO NPs' SPR spike produced using an alcoholic solution of Phoenix dactylifera was identified at 270 nm. Several elements include crystallinity, crystal size, and form. Several elements, including accumulations, can influence the SPR peaks of NPs, the amount of the metallic precursor, crystallite dimension and structure, and crystallinity. Another sign that CuO is spherical and has a reduced size is that a single spark appears on the UV curve at wavelengths under 370 nm.

3.2. DLS Examination. To analyze the usual size estimation of particles for the greenish pathway synthesized CuO NPs, the technique of dynamic light scattering (DLS) was used. The largest size of particles that could disperse, as seen in Figure 3, was 52.32 nm. This study's findings are in excellent accord with actinomycetes' artificially synthesized CuO NPs, which have a median particle dimension of 53 nm. According to previous study notifications on the biosynthesis of CuO NPs using various procedures, the CuO NPs with an erratic shape of a sphere and nanometer dimension substances are more susceptible to killing the microbes in the culture broth substance due to the combination of more surface area concentration to volume rations.

3.3. XRD Analysis. Radioactive diffraction of the chemical arrangement of CuO NPs derived from plants was discovered via XRD examination, which revealed 12 individual peaks. Bragg's diffraction peaks are frequently observed at 2Θ values

https://doi.org/10.1021/acsomega.3c05588
ACS Omega 2023, 8, 39680−39689

of 28.76, 32.3, 34.9, 37.8, 48.3, 54.6, 62.1, 69.3, 71.32, and 74.2°, which correspond to planes of (111), (110), (−111), (111), (−202), (020), (202), (−113), (−311), (220), (311), and (−222), respectively (Figure 4). Referring to the Joint Commission on Powder Diffraction (JCPD) specification having document reference 80-1268, the acquired XRD spectral data confirmed that plant CuO NPs comprised face-centered cylindrical structures and had crystalline character.[23] The creation of CuO NPs is indicated by the measured peaks at 2Θ values in the region of 35−39°, as described earlier.

The lack of extra peaks in the XRD pattern supported the exceptional purity of the synthesized CuO NPs. The observations were consistent with a range of green-synthesized CuO NP research. According to Ahmed et al., the XRD pattern's crisp and distinct Bragg's peaks show that a crystalline structure with diameters under 100 nm was successfully formed. Utilizing Debye−Scherrer's equation, the XRD structure may be used to determine the crystal dimensions of CuO NPs produced during biosynthesis. The median size of the crystallite in the present investigation was 28 nm.

3.4. FTIR Analysis. Aromatic substances' C−N bend phase generated pronounced and powerful spikes at 1107 and 1429 cm^{-1}. Because of the existence of the alkene groupings, the elevated peak at 870 cm^{-1} is attributable to the C−H resonance. CuO metal synthesis is attributed to the distinct spikes at 624, 701, and 777 cm^{-1}. Similar investigations have shown that the stretched and vibrating modes of CuO NPs match the two wavelengths of absorption spikes at 799 and 855 cm^{-1}.

Utilizing *P. guajava* extract from the leaves, the Fourier transform infrared spectrum was employed to identify biological molecules that were effective in the plant material and to ascertain the functional category interactions of synthesized CuO NPs.[24] Figure 5 depicts the FTIR structure of the produced CuO NPs, which showed several absorbance regions. The OH stretched properties of phenol compounds and alcohols corresponded to broad ranges of 2978−3740 cm^{-1} broad ranges. The additional aromatic ring's vibration patterns were allocated to the absorbent regions at 1640 and 768 cm^{-1}.

3.5. Microstructural Analysis. The morphological properties of biosynthesized CuO NPs, such as their dimensions, forms, and accumulations, are key factors impacting their biological functions. Investigations using TEM (Figure 6 (a)) and SEM (Figure 6 (b)) are effective methods for examining these characteristics. The *P. guajava* leaf-based CuO NPs are spherical, neatly organized, and devoid of agglomeration or clustering, as demonstrated. CuO NPs produced during biosynthesis ranged in size from 10 to 30 nm, with a median dimension of 23 nm. This is similar to the previous study of an aqueous solution of Soursop leaves used to create CuO NPs in a comparable work, and the median dimension of the particles ranged from 15 to 33 nm.[25]

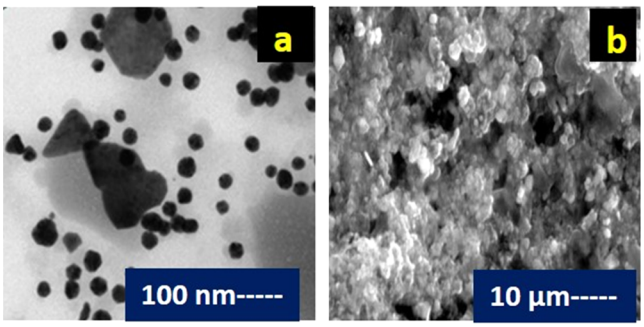

Figure 6. Microstrctural images of biosynthesized CuO nanoparticles of (a) TEM and (b) SEM.

Additionally, the seeds of pumpkin extract have shown great effectiveness in producing circle CuO NPs with a median particle size of 20 nm. The sizes and forms of nanoparticles are intimately connected with their biological function.[26] For example, CuO NPs' cytotoxic efficiency varied depending on their size, which ranged from 4 to 24 nm. Because tiny particles are more effective in dissolving hazardous ions (Cu^{2+}) than larger sizes, it was previously discovered that CuO NPs having dimensions of 24 nm were significantly harmful to adenocarcinoma cells A549 when compared with those with dimensions of 5 nm. Additionally, SEM analysis was used to look into the topographic and morphological characteristics of plant-based CuO NPs. CuO NPs were organized in a spherical form without accumulation, as is evident from their flat exterior. Similarly, SEM analysis was used to identify the spherical form of CuO NPs created by using infusions of oranges or leaves of mint. Some accumulations in SEM photos result from coating compounds made from extracts of plants that may cause them to grow larger during SEM than during TEM inspection.

3.6. Wastewater Treatment. The main difficulty many countries, especially those with water shortages, are currently experiencing is the search for alternative chemical agents that may be employed to purify diverse industrial effluents. The major causes of the hazards in these pollutants and related sewers throughout the tanning process are the overabundance of chromium ions and additional organic and inorganic substances. Improper handling of such pollutants seriously threatens the ecological system, including plants, animals, and humans.[27] Green nanotechnology provides an innovative, cost-effective way for creating new, environmentally friendly active compounds with enormous surfaces and strong stability that may be utilized to eliminate various pollutants.[28] Additionally, by eradicating harmful bacteria in wastewater, consuming active compounds with antimicrobial properties can improve the water's quality. This section examined whether the generated CuO NPs would successfully treat and decompose dyeing sewage, among the most hazardous materials produced by the leather industry.[29,30] Various CuO NP quantities (0.4, 0.8, 1.2, and 1.6 mg/mL) were used in the study for a range of periods (30−210 min with periods of 30 min). To the best of our ability, this is the first study on implementing green-synthesized CuO NPs for the discoloration and purification of crude dyeing effluent (Figure 7). According to the data analysis, removing color from the dyeing effluent by CuO NPs was concentration-dependent and dependent upon time. This result might be explained by a rise in spots for adsorption at high concentrations, which would boost the decolorization process.[31,32]

The findings are consistent with previously released research on using nanocrystals for dye in decolorization. The discoloration proportion at a lower dosage (0.4 mg/mL) during incubating conditions was 11.01 for 0.7% after 30 min and attained 35 for 0.4% after 210 min in contrast to the reference. At elevated levels, the proportions rose. For example, at doses of 0.8 and 1.2 mg/mL, the discoloration proportions remained 13.10 for 0.3% and 17.21 for 0.2% after 30 min,

https://doi.org/10.1021/acsomega.3c05588
ACS Omega 2023, 8, 39680−39689

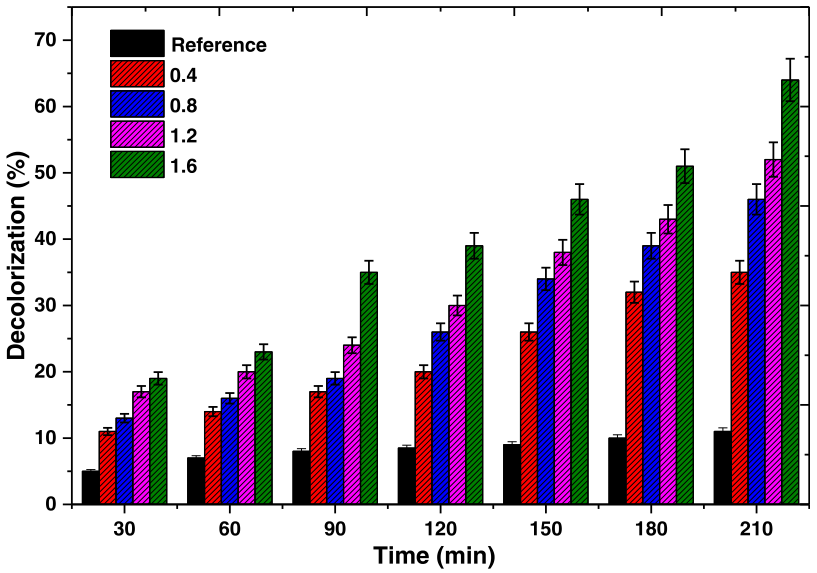

Figure 7. Decolorization proportion of wastewater processing at different concentrations (0.4, 0.8, 1.2, and 1.6 mg/ML) in dark mode.

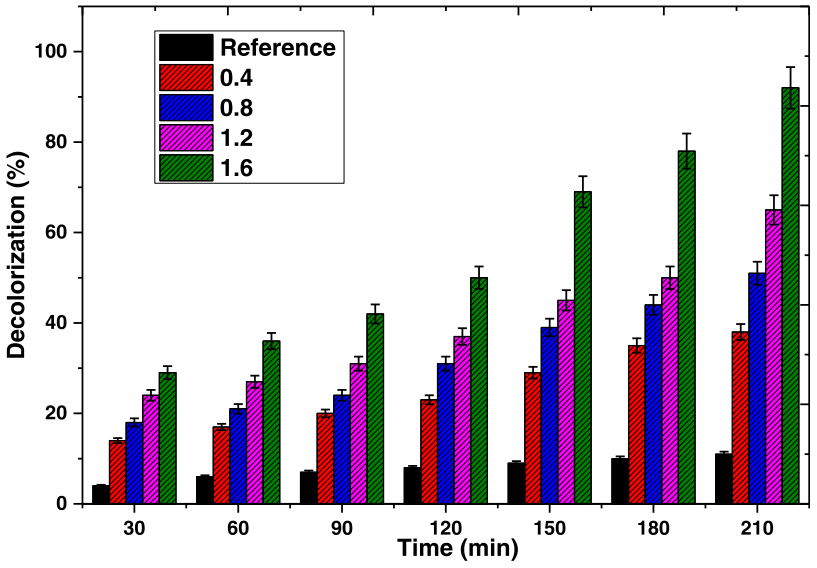

Figure 8. Decolorization proportion of wastewater processing at different concentrations (0.4, 0.8, 1.2, and 1.6 mg/mL) at sunlight conditions.

respectively, and increased to 46.30 for 0.8% and 52.36 for 1.2% after 210 min. Similar investigations found that after 30 min of being treated with green-synthesized MgO NPs at levels of 0.25, 0.50, 0.75, and 1.0 g/mL, the removal of the color of dyeing effluent was achieved with proportions of 16.2, 28.4, 37.1, and 53.6% in contrast with the control sample (1.9%). Following 180 min, these rates rose to 36.21, 53.65, 79.24, and 93.54% at the identical prior percentages.[22] In a recent investigation, after 144 min of being administered at 1.0 mg/mL, the green-synthesized Fe_2O_3 NPs exhibited a discoloration proportion of 78.21%. The greatest discoloration proportion (72.31) was observed at a concentration of 1.6% under dark conditions.[33]

The present investigation was conducted over a duration of 210 min at a dose of 1.6 mg/mL. Notably, incubating in sunlight (Figure 8) increased the discoloration of dyeing effluent utilizing plant-based CuO NPs. The decolorization proportions rose from 14.30% after 30 min at a dose of 0.4 mg/mL to 38.52% following 210 min at the identical level according to an evaluation of deviation. At doses of 0.8, 1.2, and 1.6 mg/mL following 210 min, the greatest discoloration proportions during light illumination conditions were 51.10, 65.17, and 92.21%, respectively. The lower CuO NPs enhanced the outermost area and thus the number of adsorption sites. As a result, higher CuO NP levels led to the greatest discoloration proportions. The enhancement of waste material discoloration and processing in sunlight may be attributed to the light stimulation of the electrons on the outermost layer of CuO NPs, which in turn results in the generation of pairs of electrons−holes (e^-CB and h^+VB) by transferring electrons from the valence band (VB) to the conduction band (CB). Superoxides ($^{\bullet}O^{2-}$) and hydrogen peroxide ($^{\bullet}$OOH) formed when energized e^- in the CB interacted with oxygen, while unstable hydroxide radicals ($^{\bullet}$OH) were created when h^+ reacted with water.[34,35] In sewage, such unstable molecules react with impurities and dyes, degrading them to carbon dioxide, water, and other tiny ions. According to the information gathered, the physical and

https://doi.org/10.1021/acsomega.3c05588
ACS Omega 2023, 8, 39680−39689

chemical traits of sun exposure wastewater have been investigated at an amount of 1.6 mg/mL, following 210 min of exposure to sunlight illnesses, which was identified as the most effective condition for the decolorization process.[36]

Compared to natural wastewater, the effluent variables pH, COD, BOD, TSS, TDS, and resistivity were assessed under ideal conditions. The range of contaminants found in tannery effluent depends on the dimension of the tanning box, the substances employed, the finished goods, and the volume of water utilized throughout the tanning procedure. Significant COD, BOD, TDS, saltiness, TSS, conductance, sulfides, and toxic metals frequently constitute the key characteristics of dyeing effluent. This discovery may be connected to using numerous substances, including chlorine, magnesium, bicarbonates, phosphorus, phosphate sulfurates, mineral salts, nitrates, and water-soluble salts, throughout the production of leatherette. According to the results, the green-synthesized CuO NPs were effective in reducing the physical properties of tanned effluent by, accordingly, 93.24, 88.62, 94.21, 87.5, and 98.3% for COD, BOD, TSS, and conductance. The overabundance of bicarbonate elements and calcium carbonate throughout leather dyeing procedures may be to blame for the alkaline surroundings of the unsophisticated dyeing effluent. In this section, the CuO NP treatments reduced the pH readings from 8.3 0.3 to 7.2 due to the drop in pollutant concentrations. It may be said that the green-synthesized CuO NPs thus constitute a potential bioadsorbent for different pollutants in sewage.[37] Magnetite nanomaterials may reduce the COD value of the dyeing effluent between 5081 and 584 mg/L with an efficiency of 87.14%. According to Zhang et al., low levels of CuO NPs (1 mg/L) are thought to be of greater promise than large amounts (30 and 50 mg/L), which can impede the growth of bacteria. According to Wang et al., declining the removal of COD rates throughout sewage treatment at both low and high CuO NP amounts was not of statistical significance. According to the previous study, the elimination amount of COD utilizing 0.1 mg/L CuO NPs was 93.21%, but when its concentration was increased to 20 mg/L, the figure dropped to 88.25%.[36]

4. CONCLUSIONS

The *P. guajava* leaf extract was used in this study to effectively produce CuO NPs via the environmental route. This represents the first time that environmentally friendly chemistry has been used in the cultivation of this plant to produce CuO NPs. Because of botanical chemicals, whose phytocomponents are called capping, decreasing, and stabilizing agents of CuO NPs, the natural chemical method of CuO NP synthesis is less harmful and more efficient. The biological molecules that facilitated the production of CuO NPs and their crystal shapes need to be validated. The suggested approach for biosynthesizing CuO NPs was physiochemically characterized by FTIR and XRD spectra. SEM and TEM images demonstrated the surface structure of the spheres and forms, and a recommended range was around 40−150 nm. Additionally, DLS was used to validate the median particle size. The catalytic properties of CuO NPs in total darkness resulted in a 72.31% discoloration, whereas exposure to sunshine increased the nanomaterials' catalyst performance to 87.5%. By lowering Co, Pb, Ni, Cd, and Cr(VI) in sewage by 73.2, 80.8, 72.4, 64.4, and 91.4%, CuO NP demonstrated its effectiveness as a nanosorbent. TSS, TDS, COD, BOD, and conductance were successfully reduced by nanotreatment of tanning effluent, with proportion reductions of 93.24, 88.62, 94.21, 87.5, and 98.3%, respectively.

■ ASSOCIATED CONTENT

Data Availability Statement

The data used to support the findings of this study are included in the article. Should further data or information be required, these are available from the corresponding author upon request.

■ AUTHOR INFORMATION

Corresponding Author

Prabhu Paramasivam − *Department of Mechanical Engineering, College of Engineering and Technology, Mettu University, Metu 318, Ethiopia;* orcid.org/0000-0002-2397-0873; Email: prabhu.paramasivam@meu.edu.et, lptprabhu@gmail.com

Authors

Natrayan Lakshmaiya − *Department of Mechanical Engineering, Saveetha School of Engineering, SIMATS, Chennai, Tamil Nadu 602 105, India*

Raviteja Surakasi − *Department of Mechanical Engineering, Lendi Institute of Engineering and Technology, Vizianagaram, Andhra Pradesh 535005, India*

V. Swamy Nadh − *Department of Civil Engineering, Aditya College of Engineering, Surampalem, Andhra Pradesh 533437, India*

Chidurala Srinivas − *Department of Mechanical Engineering, Vaageswari College of Engineering, Karimnagar, Telangana 505527, India*

Seniappan Kaliappan − *Department of Mechatronics Engineering, KCG College of Technology, Chennai, Tamil Nadu 600097, India*

Velmurugan Ganesan − *Institute of Agricultural Engineering, Saveetha School of Engineering, SIMATS, Chennai, Tamil Nadu 602 105, India*

Seshathiri Dhanasekaran − *Department of Computer Science, UiT The Arctic University of Norway, Tromso 9037, Norway;* orcid.org/0000-0003-0624-1991

Complete contact information is available at: https://pubs.acs.org/10.1021/acsomega.3c05588

Notes

The authors declare no competing financial interest.

■ ACKNOWLEDGMENTS

The authors thank Saveetha School of Engineering, Chennai, for supporting this research and Mattu University, Ethiopia, for their extended support on this publication process.

■ REFERENCES

(1) Singh, P.; Yadav, S. K.; Kuddus, M.Green nanomaterials for wastewater treatment. In *Green Nanomaterials: Processing, Properties, and Applications*; Springer, 2020; Vol. *126*, pp 227−242.

(2) El-Gendy, N. S.; Nassar, H. N. Biosynthesized magnetite nanoparticles as an environmental opulence and sustainable wastewater treatment. *Sci. Total Environ.* **2021**, *774*, No. 145610.

(3) Rafique, M.; Shafiq, F.; Gillani, S. S. A.; Shakil, M.; Tahir, M. B.; Sadaf, I. Eco-friendly green and biosynthesis of copper oxide nanoparticles using Citrofortunella microcarpa leaves extract for efficient photocatalytic degradation of Rhodamin B dye form textile wastewater. *Optik* **2020**, *208*, No. 164053.

(4) Ahmed, A.; Usman, M.; Yu, B.; Ding, X.; Peng, Q.; Shen, Y.; Cong, H. Efficient photocatalytic degradation of toxic Alizarin yellow R dye from industrial wastewater using biosynthesized Fe nanoparticle and study of factors affecting the degradation rate. *J. Photochem. Photobiol., B* **2020**, *202*, No. 111682.
(5) Jeevanandam, J.; Manchala, S.; Danquah, M. K. Wastewater Treatment by Photocatalytic Biosynthesized Nanoparticles. In *Handbook of Nanomaterials and Nanocomposites for Energy and Environmental Applications*; Springer, 2020; pp 1−23.
(6) Giri, A. K.; Kumar, V.; Vyas, V.; Kumar, A.; Gautam, D. Phytoremediation of Domestic Sewage in Constructed Wetland Integrated with Cultivation of Chlorella sp.: A Novel Technique for Remediation and Resource Recovery. *Asian J. Water, Environ. Pollut.* **2023**, *20*, 91−98.
(7) Bilal, H.; Raza, H.; Sarfaraz, S.; Khan, D. H. Endophytic Potential of Entomopathogenic Fungi for the Remediation of Wastewater. *J. Bioresour. Manage.* **2023**, *10*, No. 6.
(8) Yuan, D.; Wang, L.; Wang, H.; Miao, R.; Wang, Y.; Jin, H.; Tan, L.; Wei, C.; Hu, Q.; Gong, Y. Application of microalgae Scenedesmus acuminatus enhances water quality in rice-crayfish culture. *Front. Bioeng. Biotechnol.* **2023**, *11*, No. 1143622.
(9) Epelle, E. I.; Macfarlane, A.; Cusack, M.; Burns, A.; Okolie, J. A.; Mackay, W.; Rateb, M.; Yaseen, M. Ozone application in different industries: A review of recent developments. *Chem. Eng. J.* **2023**, *454*, No. 140188.
(10) Govindaraj, V.; Murugan, K.; Baskar, P.; Sathaiya, J. Treatment of Dairy Wastewater and Sludge Production Using Algae Bio Reactor. *Asian J. Water, Environ. Pollut.* **2023**, *20*, 77−83.
(11) Pérez-Aguilar, H.; Lacruz-Asaro, M.; Ruzafa-Silvestre, C.; Arán-Ais, F. Protein recovery from wastewater animal processing by-products of rendering plants for biostimulant applications in agriculture. *Sustainable Chem. Pharm.* **2023**, *32*, No. 101009.
(12) Yusof, M. A. B. M.; Chan, Y. J.; Chong, C. H.; Chew, C. L. Effects of Operational Processes and Equipment in Palm Oil Mills on Characteristics of Raw Palm Oil Mill Effluent (POME): A Comparative Study of Four Mills. *Cleaner Waste Syst.* **2023**, *5*, No. 100101, DOI: 10.1016/j.clwas.2023.100101.
(13) Swapnil, P.; Singh, L. A.; Mandal, C.; Sahoo, A.; Batool, F.; Meena, M.; Kumari, P.; Zehra, A.; et al. Functional characterization of microbes and their association with unwanted substance for wastewater treatment processes. *J. Water Process Eng.* **2023**, *54*, No. 103983.
(14) Saim, A. K.; Adu, P. C. O.; Amankwah, R. K.; Oppong, M. N.; Darteh, F. K.; Mamudu, A. W. Review of catalytic activities of biosynthesized metallic nanoparticles in wastewater treatment. *Environ. Technol. Rev.* **2021**, *10*, 111−130.
(15) Hasan, K. M. F.; Horváth, P. G.; Horváth, A.; Alpár, T. Coloration of woven glass fabric using biosynthesized silver nanoparticles from Fraxinus excelsior tree flower. *Inorg. Chem. Commun.* **2021**, *126*, No. 108477.
(16) Makofane, A.; Motaung, D. E.; Hintsho-Mbita, N. C. Photocatalytic degradation of methylene blue and sulfisoxazole from water using biosynthesized zinc ferrite nanoparticles. *Ceram. Int.* **2021**, *47*, 22615−22626.
(17) Hassan, E.; Gahlan, A. A.; Gouda, G. A. Biosynthesis approach of copper nanoparticles, physicochemical characterization, cefixime wastewater treatment, and antibacterial activities. *BMC Chem.* **2023**, *17*, No. 71, DOI: 10.1186/s13065-023-00982-7.
(18) Fan, Y.; Su, J.; Xu, L.; Liu, S.; Hou, C.; Liu, Y.; Cao, S. Removal of oxytetracycline from wastewater by biochar modified with biosynthesized iron oxide nanoparticles and carbon nanotubes: Modification performance and adsorption mechanism. *Environ. Res.* **2023**, *231*, No. 116307, DOI: 10.1016/j.envres.2023.116307.
(19) Yang, K.; Liu, M.; Weng, X.; Owens, G.; Chen, Z. Fenton-like oxidation for the simultaneous removal of estrone and β-estradiol from wastewater using biosynthesized silver nanoparticles. *Sep. Purif. Technol.* **2022**, *285*, No. 120304.
(20) Vitor, G.; Palma, T. C.; Vieira, B.; Lourenço, J. P.; Barros, R. J.; Costa, M. C. Start-up, adjustment and long-term performance of a two-stage bioremediation process, treating real acid mine drainage, coupled with biosynthesis of ZnS nanoparticles and ZnS/TiO2 nanocomposites. *Miner. Eng.* **2015**, *75*, 85−93.
(21) Manivasagan, P.; Kang, K.-H.; Kim, D. G.; Kim, S.-K. Production of polysaccharide-based bioflocculant for the synthesis of silver nanoparticles by Streptomyces sp. *Int. J. Biol. Macromol.* **2015**, *77*, 159−167.
(22) Fouda, A.; Hassan, S. E-D.; Saied, E.; Hamza, M. F. Photocatalytic degradation of real textile and tannery effluent using biosynthesized magnesium oxide nanoparticles (MgO-NPs), heavy metal adsorption, phytotoxicity, and antimicrobial activity. *J. Environ. Chem. Eng.* **2021**, *9*, No. 105346.
(23) Santhoshkumar, T.; Rahuman, A. A.; Jayaseelan, C.; Rajakumar, G.; Marimuthu, S.; Kirthi, A. V.; Velayutham, K.; Thomas, J.; Venkatesan, J.; Kim, S.-K. Green synthesis of titanium dioxide nanoparticles using *Psidium guajava* extract and its antibacterial and antioxidant properties. *Asian Pac. J. Trop. Med.* **2014**, *7*, 968−976.
(24) He, K.; Chen, G.; Zeng, G.; Huang, Z.; Guo, Z.; Huang, T.; Peng, M.; Shi, J.; Hu, L. Applications of white rot fungi in bioremediation with nanoparticles and biosynthesis of metallic nanoparticles. *Appl. Microbiol. Biotechnol.* **2017**, *101*, 4853−4862.
(25) Pelegrino, M. T.; Kohatsu, M. Y.; Seabra, A. B.; Monteiro, L. R.; Gomes, D. G.; Oliveira, H. C.; Rolim, W. R.; de Jesus, T. A.; Batista, B. L.; Lange, C. N. Effects of copper oxide nanoparticles on growth of lettuce (Lactuca sativa L.) seedlings and possible implications of nitric oxide in their antioxidative defense. *Environ. Monit. Assess.* **2020**, *192*, No. 232, DOI: 10.1007/s10661-020-8188-3.
(26) Tabrez, S.; Khan, A. U.; Hoque, M.; Suhail, M.; Khan, M. I.; Zughaibi, T. A. Biosynthesis of ZnO NPs from pumpkin seeds′ extract and elucidation of its anticancer potential against breast cancer. *Nanotechnol. Rev.* **2022**, *11*, 2714−2725.
(27) Garole, V. J.; Choudhary, B. C.; Tetgure, S. R.; Garole, D. J.; Borse, A. U. Detoxification of toxic dyes using biosynthesized iron nanoparticles by photo-Fenton processes. *Int. J. Environ. Sci. Technol.* **2018**, *15*, 1649−1656.
(28) Liu, J.; Pemberton, B.; Scales, P. J.; Martin, G. J. O. Ammonia tolerance of filamentous algae Oedogonium, Spirogyra, Tribonema and Cladophora, and its implications on wastewater treatment processes. *Algal Res.* **2023**, *72*, No. 103126.
(29) El-Aswar, E. I.; Zahran, M. M.; El-Kemary, M. Optical and electrochemical studies of silver nanoparticles biosynthesized by Haplophyllum tuberculatum extract and their antibacterial activity in wastewater treatment. *Mater. Res. Express* **2019**, *6*, No. 105016.
(30) Waghmode, M. S.; Gunjal, A. B.; Mulla, J. A.; Patil, N. N.; Nawani, N. N. Studies on the titanium dioxide nanoparticles: Biosynthesis, applications and remediation. *SN Appl. Sci.* **2019**, *1*, No. 310, DOI: 10.1007/s42452-019-0337-3.
(31) Vo, T.-T.; Nguyen, T. T-N.; Huynh, T. T-T.; Vo, T. T-T.; Nguyen, T. T-N.; Nguyen, D.-T.; Dang, V.-S.; Dang, C.-H.; Nguyen, T.-D. Biosynthesis of silver and gold nanoparticles using aqueous extract from Crinum latifolium leaf and their applications forward antibacterial effect and wastewater treatment. *J. Nanomater.* **2019**, *2019*, 1−14.
(32) Nwanya, A. C.; Razanamahandry, L. C.; Bashir, A. K. H.; Ikpo, C. O.; Nwanya, S. C.; Botha, S.; Ntwampe, S. K. O.; Ezema, F. I.; Iwuoha, E. I.; Maaza, M. Industrial textile effluent treatment and antibacterial effectiveness of Zea mays L. Dry husk mediated bio-synthesized copper oxide nanoparticles. *J. Hazard. Mater.* **2019**, *375*, 281−289.
(33) Fouda, A.; Hassan, S. E-D.; Saied, E.; Azab, M. S. An eco-friendly approach to textile and tannery wastewater treatment using maghemite nanoparticles (γ-Fe2O3-NPs) fabricated by Penicillium expansum strain (Kw). *J. Environ. Chem. Eng.* **2021**, *9*, No. 104693.
(34) Acosta, E. A. C.; Juárez, H. D. G.; Marchena, A. M.; García, I. E. S. Efficiency of a wastewater treatment system in a tannery industry. *Adv. Water Sci.* **2023**, *34*, 45−53.
(35) Tan, Y. H.; Chai, M. K.; Na, J. Y.; Wong, L. S. Microalgal Growth and Nutrient Removal Efficiency in Non-Sterilised Primary

Domestic Wastewater. *Sustainability* **2023**, *15*, No. 6601, DOI: 10.3390/su15086601.
(36) Eid, A. M.; Fouda, A.; Hassan, S. E. D.; Hamza, M. F.; Alharbi, N. K.; Elkelish, A.; Alharthi, A.; Salem, W. M. Plant-Based Copper Oxide Nanoparticles; Biosynthesis, Characterization, Antibacterial Activity, Tanning Wastewater Treatment, and Heavy Metals Sorption. *Catalysts* **2023**, *13*, No. 348, DOI: 10.3390/catal13020348.
(37) Sathiyavimal, S.; Vasantharaj, S.; Veeramani, V.; Saravanan, M.; Rajalakshmi, G.; Kaliannan, T.; Al-Misned, F. A.; Pugazhendhi, A. Green chemistry route of biosynthesized copper oxide nanoparticles using *Psidium guajava* leaf extract and their antibacterial activity and effective removal of industrial dyes. *J. Environ. Chem. Eng.* **2021**, *9*, No. 105033.

https://doi.org/10.1021/acsomega.3c05588
ACS Omega 2023, 8, 39680−39689